



HAL
open science

500–2000-MHz Airborne Brightness Temperature Measurements Over the East Antarctic Plateau

Marco Brogioni, Marion Leduc-Leballeur, Mark J Andrews, Giovanni Macelloni, Joel T Johnson, Kenneth C Jezek, Caglar Yardim

► **To cite this version:**

Marco Brogioni, Marion Leduc-Leballeur, Mark J Andrews, Giovanni Macelloni, Joel T Johnson, et al.. 500–2000-MHz Airborne Brightness Temperature Measurements Over the East Antarctic Plateau. IEEE Geoscience and Remote Sensing Letters, 2022, 19, pp.7001005. 10.1109/lgrs.2021.3056740 . hal-03719107

HAL Id: hal-03719107

<https://hal.science/hal-03719107>

Submitted on 10 Jul 2022

HAL is a multi-disciplinary open access archive for the deposit and dissemination of scientific research documents, whether they are published or not. The documents may come from teaching and research institutions in France or abroad, or from public or private research centers.

L'archive ouverte pluridisciplinaire **HAL**, est destinée au dépôt et à la diffusion de documents scientifiques de niveau recherche, publiés ou non, émanant des établissements d'enseignement et de recherche français ou étrangers, des laboratoires publics ou privés.

500–2000-MHz Airborne Brightness Temperature Measurements Over the East Antarctic Plateau

Marco Brogioni, Marion Leduc-Leballeur, Mark J. Andrews, Giovanni Macelloni, Joel T. Johnson, Kenneth C. Jezek, Caglar Yardim

Abstract—Measurements of the 500–2000-MHz brightness temperature spectra of Antarctica acquired under the Ice Sheet and Sea Ice Ultrawideband Microwave Airborne eXperiment (ISSIUMAX) are reported. These data sets support the remote sensing of ice sheet properties, in particular information on the temperature profile within the ice sheet. The Ultrawideband Software-Defined Microwave Radiometer (UWBRAD) was installed on a Twin Otter aircraft, and measurements were collected on coastal areas and the interior of East Antarctica in November and December 2018. UWBRAD 500–2000-MHz brightness temperature measurements along a 1000-km path over the ice sheet are compared in this letter to forward model simulations for these locations and confirm the expected sensitivities to ice sheet parameters.

Index Terms—Cryosphere, ice sheet, passive microwave.

I. INTRODUCTION

COLD regions are a major element of the Earth system. They are subject to global scale dynamics, and also impact important processes that control or modulate global water, heat, energy, and chemistry budgets. Passive microwave sensors operating at C-band and above have made important contributions to monitoring Earth’s cold regions, and the availability of L-band (1.4 GHz) observations over the last decade from missions such as the European Space Agency (ESA)’s Soil Moisture and Ocean Salinity (SMOS) from 2009, the National Aeronautical and Space Agency (NASA)’s Aquarius from 2011 to 2015 and NASA’s Soil Moisture Active Passive (SMAP) from 2015 have opened a new era in cryospheric remote sensing.

The interest in L-band for snow and ice applications arises from the very low attenuation rate in ice at this frequency and the low level of scattering from medium inhomogeneities (e.g., snow grain size and bubbles in ice) due to their small size compared to the electromagnetic wavelength. Consequently, in dry snow and continental ice, the penetration depth is very high

(reaching up to several hundreds of meters), opening opportunities for probing internal properties of ice sheets. Studies demonstrate that it is possible to estimate temperature profiles over a wide region of Antarctica using SMOS observations combined with microwave emission and glaciological models [1]. However, it was found difficult to estimate the temperature at depths greater than 2000 m due to the limited penetration depth at L-band.

Recent analyses have shown the potential to overcome these limitations by using measurements over the 500–2000-MHz range [2], [3], [4]. The Ultrawideband Software-Defined Microwave Radiometer (UWBRAD) funded through NASA’s Instrument Incubator Program was developed to demonstrate this concept [5]. Two airborne campaigns in Greenland (September 2016 and 2017) demonstrated the feasibility to collect brightness temperature observations even in the 500–2000-MHz frequency range that is largely not protected from radio frequency interference (RFI) [6].

In this letter, we present UWBRAD measurements over Antarctica performed during the “Ice Sheet and Sea Ice Ultrawideband Microwave Airborne eXperiment” (ISSIUMAX) funded by the Italian Programme of National Research in Antarctica (PNRA). This is the first campaign carried out in Antarctica for collecting wideband brightness temperature measurements in the 500–2000-MHz range. Section II describes the field experiment and the instrument. Section III then presents the measurements collected over the ice sheet and compares them with forward model predictions. Final conclusions are provided in Section IV.

II. THE ISSIUMAX PROJECT

A. Field Experiment Description

The ISSIUMAX campaign took place during the austral summer 2018 in East Antarctica; airborne measurements were performed along about 5000 km spread over four flights (see Fig. 1). The flight lines surveyed ice shelves, glaciers, snow-covered land, sea ice and, ice-free ocean near Mario Zucchelli Station (MZS, 74.69°S, 164.11°E) in Terra Nova Bay, as well as the ice sheet between MZS and Concordia Station (75.10°S, 123.33°E) and the Dome C area on the East Antarctic Plateau.

MZS is located in a rocky coastal area facilitating access by supply ships, the maintenance of the station, and the operation of several airstrips. PNRA provides all the facilities for aircraft and helicopter maintenance, air traffic coordination in the region, berthing, and other logistical support. Moreover, the milder climate at MZS compared to other stations such

Manuscript received October 19, 2020; revised December 14, 2020; accepted January 29, 2021.

The results from the UWBRAD system were supported in part by the NASA’s Instrument Incubator Program under Grant NNX14AE68G, in part by the Cryospheric Science Program under Grant 80NSSC18K0550 and Grant NNX14AH91G, and in part by the National Science Foundation under Grant 1838401. The Antarctic campaign was supported by the Italian Antarctic Programme—PNRA under Grant 2016/AZ3.02.

M. Brogioni, M. Leduc-Leballeur, and G. Macelloni are with the Institute of Applied Physics Nello Carrara, National Research Council, Florence, Italy (e-mail: m.brogioni@ifac.cnr.it).

M. J. Andrews, J. T. Johnson, and C. Yardim are with the ElectroScience Laboratory, The Ohio State University, Columbus, OH 43210 USA.

K. C. Jezek is with the Byrd Polar Research Center, The Ohio State University, Columbus, OH 43210 USA.

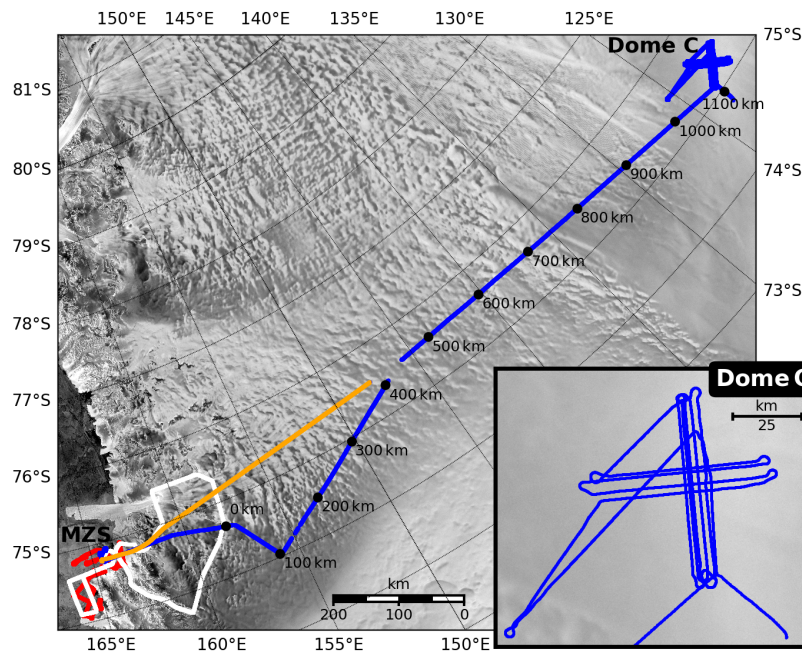


Fig. 1. UWBRAD flight lines on November 24 (red and white), December 3 (blue), and December 5 (orange) overlaid on a RADARSAT-1 SAR image mosaic [7]. The flight going from the MZS to the Concordia Station (Dome C) is marked at every 100 km covered.

as Concordia facilitates the deployment of instruments on aircraft.

The UWBRAD radiometer was installed aboard a Twin Otter aircraft operated by Kenn Borek Air Ltd. On November 24, 2018, a first flight was performed over the coastal region around MZS. It traversed sea-ice cover and open-water polynya, which are observed at the beginning and at the end of the flight for calibration purposes, as well as the Nansen ice shelf, Priestly, and David glaciers. On December 3, a flight traversed from MZS to Dome C and included a set of closely spaced tracks over Little Dome C (75.5°S , 122.3°E). On December 5, the expedition crew returned to MZS and collected observations on the second half of the flight and over the open sea, again for calibration purposes.

The analysis reported here focuses on the December 3 flight, which includes transit from MZS to Dome C and survey lines near Dome C.

B. Radiometer description

The UWBRAD microwave radiometer is designed to provide nadir circularly polarized brightness temperature observations over the 500–2000-MHz range using multiple-frequency channels. Because this frequency range is not a protected portion of the spectrum, the measurements can be affected by anthropogenic RFI. To address this issue, UWBRAD includes RFI detection and filtering methods that include the measurements of a spectrogram in each of 12–88 MHz channels that are resolved at 0.24-MHz frequency resolution and 1-ms time resolution so that RFI detection can be performed using time- and frequency-domain methods. The signal kurtosis is also measured and used in RFI filtering. This process allows the retention of spectrum suitable for radiometric observations even in the presence of other transmitting sources,

although some evidence of RFI remains in some cases even in the filtered data. Further technical details on the instrument are provided in [5], and additional information on the RFI environment observed is available in [8]. For the flight path considered in this letter, UWBRAD was able to estimate scene brightness temperatures for $\sim 95\%$ of the observations made following RFI filtering.

UWBRAD data are calibrated using a two-stage process. The first stage is the internal calibration described in [5], in which multiple internal calibration sources including a temperature-monitored referenced load and a noise diode source are observed and used to estimate the UWBRAD “antenna temperature” through calibration coefficients derived in preflight testing. The second involves external calibration to compensate for losses in the UWBRAD antenna, antenna cable, and other components that precede the internal calibration sources. For the ISSIUMAX campaign, this calibration linearly rescales the internally calibrated “antenna temperature” (to account for the antenna efficiency and loss) and incorporates corrections proportional to measurements from thermistors within the antenna, on the antenna cable, and on the instrument front end components (a total of five calibration coefficients—the gain and slope for the linear rescaling and constant scale factors for the three thermistor readings). These coefficients are determined through a least-squares fitting process using observations of external targets whose brightness temperature can be modeled. The latter include open-water observations as well as “crossovers” that occur when the same location is observed on multiple occasions within the campaign. A “two-scale” model of sea surface emission [9] is used for the open-water “truth” values, using estimated wind speed, salinity, and sea surface temperature values for these observations. A final calibration target included in this process

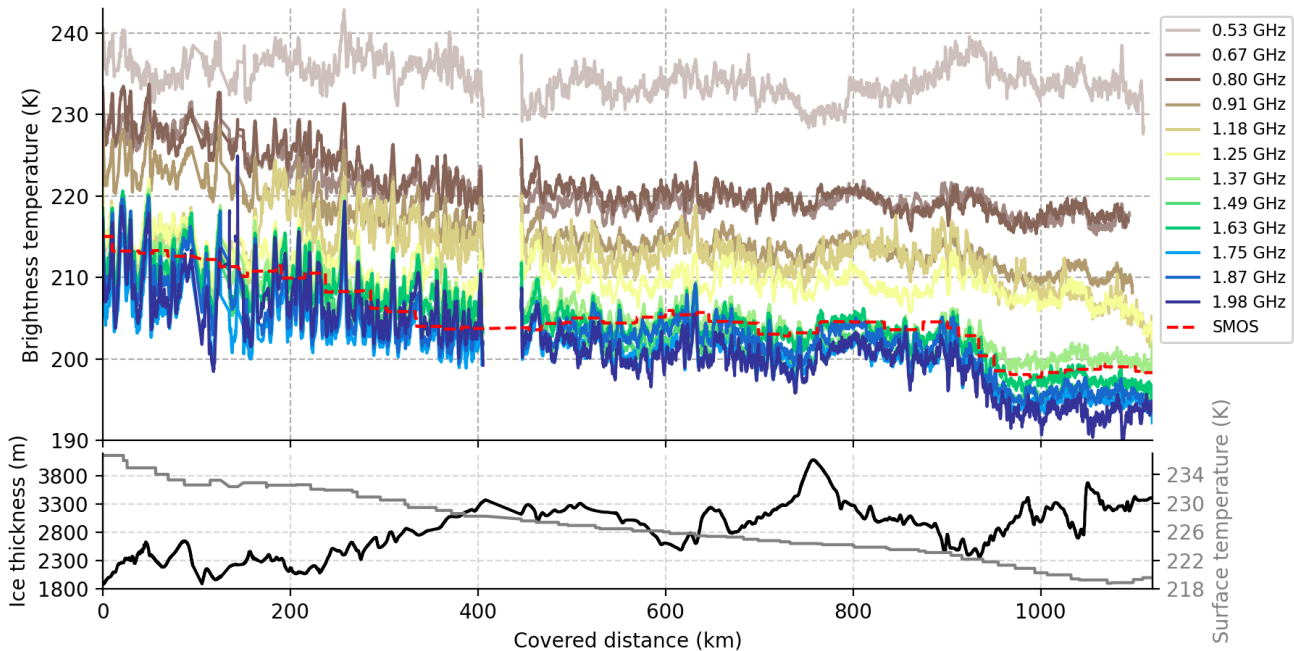


Fig. 2. (top) Twelve-channel UWB RAD brightness temperature (K) along the flight from the coast to Dome C (cf. map on Fig. 1); SMOS observations are the red dotted line; (bottom) the ice thickness (black, left axis) and surface temperature (grey, right axis).

is the mean value of forward model predictions under the Wave Approach for LOW-frequency Microwave emission in Snow (WALOMIS) forward model [10] over the Dome C flight lines that are described in Section II-C. This step was taken in order to provide a viable “hot” target to complement the “cold” target of the open ocean measurement, due to the fact that no other such targets were available within the flight for which brightness temperatures could be assumed known. While this step, therefore, should enforce the agreement between the mean value of UWB RAD measurements and the mean value of forward model predictions over the Dome C region, the relative variations of each channel over these flights remain available for inferring information on ice sheet properties. The identification of other targets suitable for the “hot” load remains under investigation so that this step can be avoided in future analyses.

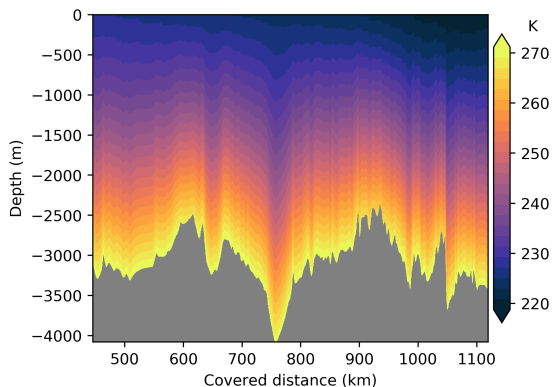


Fig. 3. Temperature profiles (K) from the Robin model along flight from distances 445–1119 km.

C. SMOS observations

SMOS observations at 1410 MHz are also used for comparison with the closest UWB RAD frequency at 1370 MHz. SMOS brightness temperatures come from the Level 3 product on a 25-km grid resolution [11] (available on <http://catds.fr>). SMOS data were obtained by averaging vertically and horizontally polarized results at incidence angle 20° in order to approximate UWB RAD’s nadir observations. Modeling studies show that the difference between true nadir results and the average of vertical and horizontal polarization at 20° incidence angle should be 0.8 K or less.

III. ANALYSIS

Fig. 2 plots UWB RAD brightness temperatures over the more than 1000-km path for the 12 frequency channels obtained from MZS to Dome C (see Fig. 1). Except at 530 MHz, a linearly decreasing trend in brightness temperature is observed from the coast to Dome C between 7 and 16 K depending on the frequency. A decrease of 13.7 K is also seen on the SMOS observations, comparable to the 1370-MHz UWB RAD decrease of 14.1 K. The SMOS signal variations are usually in agreement with the UWB RAD variations but show smoother variations in space due to the coarse spatial resolution of the SMOS grid product (25-km grid resolution) compared to that of UWB RAD ($\sim 1 \text{ km}^2$). Brightness temperatures over the UWB RAD frequency band vary by more than 30 K, which is similar to the spectra observed over the interior of the Greenland ice sheet [6]. However, a direct comparison of these results was not performed due to the differing expected temperature profiles in the Antarctic and Greenland locations observed.

Along the flight line, the snow surface temperature [12] cools approximately 18 K between the coast and Dome C area

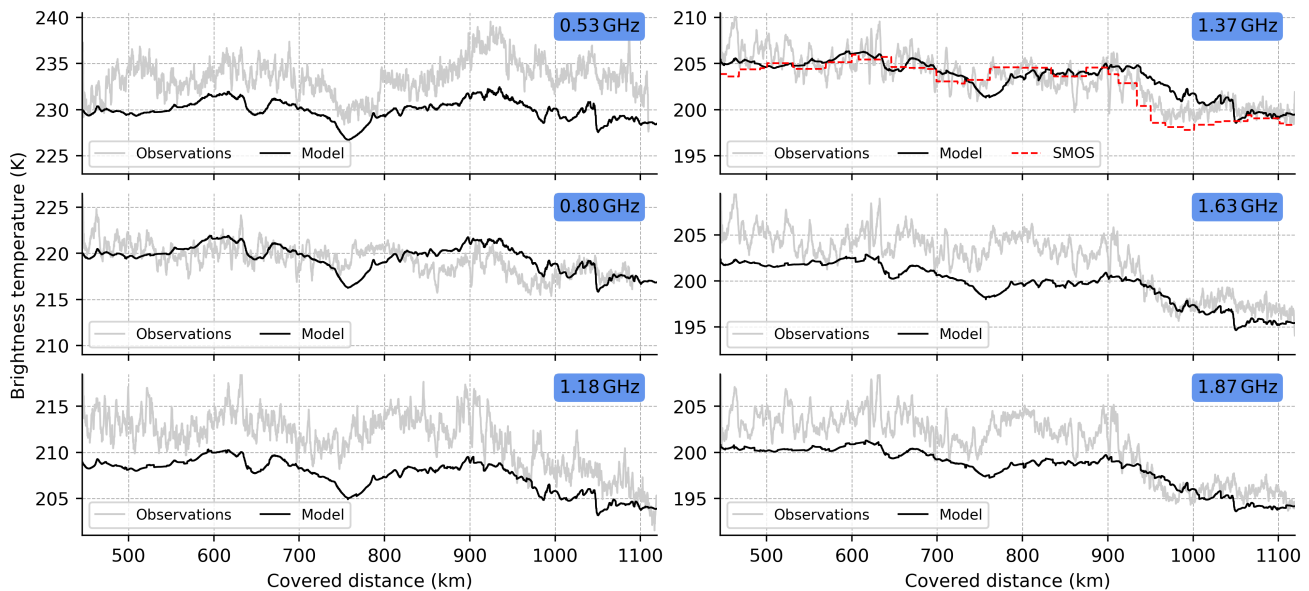


Fig. 4. Brightness temperature (K) along flight between the 445th and 1119th km for six frequencies from UWBRAD observations (grey lines) and adjusted simulations (black lines); SMOS observations are in red dotted line.

(see Fig. 2, bottom). In parallel, the ice thickness [13] increases from 1800 m near the coast to 3300 m after 400 km and then oscillates between 2500 and 4000 m as Dome C is approached.

The 1-D analytical model proposed by Robin [14] was used to estimate the ice sheet temperature profile along the flight. This model is in good agreement with the in situ temperature profile measured at Dome C (details about the model and its validation can be found in [15]). It requires four input parameters: surface snow temperature [12], ice thickness [13], snow accumulation rate [16], and geothermal heat flux [17]. Note that this model should be used only in regions with very slow horizontal ice drift, which are located along the flight line from distances 445–1119 km. Fig. 3 plots the temperature profiles estimated at locations where the Robin model should be valid.

Correlation between the 12 UWBRAD channels and the mean ice temperature between 0- and 500-m depth shows a clear link between the UWBRAD brightness temperature and the top ice temperature, except at 530 MHz where no significant correlation appears. However, this frequency is more correlated with the ice temperature at depth (i.e., average for the 1500–2000-m depth). This highlights the clear sensitivity of these frequencies to the temperature profile and the difference between higher frequencies and 530 MHz, which is mainly sensitive to the temperature at depth.

Brightness temperatures were estimated from the Robin profiles using WALOMIS [10]. WALOMIS is a coherent model based on [18], [19], originally implemented to investigate L-band brightness temperatures but here extended to the 500–2000-MHz range. Note that a bias of 6.1 K between SMOS observations and WALOMIS simulations has been reported in previous studies at Dome C. This bias has been interpreted as arising due to uncertainties in the ice dielectric constant model used or due to other effects such as surface roughness or density heterogeneity in the firn (e.g., buried

sastrugi) [15], [10]. Here, WALOMIS simulations have been corrected by removing 6.1 K over all frequencies. Applying the same bias over the whole frequency range is a significant assumption; future work will examine this assumption in further detail.

Fig. 4 compares UWBRAD observations and WALOMIS simulations for six frequency channels. At 1370 MHz, observations are in good agreement with SMOS, with a root mean square error (RMSE) of 1.71 K. These results in Fig. 4 shows a high correlation between WALOMIS model predictions and UWBRAD observations on this flight path, including the distinct difference in trends along the path between measurements at 530 MHz (which are sensitive to temperatures at greater depths) and those at higher frequencies. The RMSE between WALOMIS predictions and UWBRAD measurements varies between 1.6 and 5.8 K according to the frequency. The generally good agreement between measurements and model predictions shows that the model is capturing the dominant ice sheet properties that impact 500–2000-MHz brightness temperatures in this region, although the frequency-dependent biases observed remain a subject for continued investigation.

Survey lines near Dome C cover approximately 1000 km of flight, although much of this distance is on a tight raster (Fig. 1, zoom box). Fig. 5 (left) shows the superposition of all ice temperature profiles along the Dome C flight. The snow surface temperature is homogeneous (218.5 ± 0.3 K), but the ice thickness is more variable at 3055.6 ± 234.0 m on average and reaches about 3800 m. Fig. 5 (right) shows the mean spectrum measured by UWBRAD in this area (which is set in the calibration process to match that predicted by the model) in the 12 UWBRAD frequency channels. The standard deviation of the single frequencies varies from 1.2 to 2.9 K. This variability is included within the range provided by the WALOMIS simulations obtained with the warmest and the coldest temperature profiles. This highlights the good stability

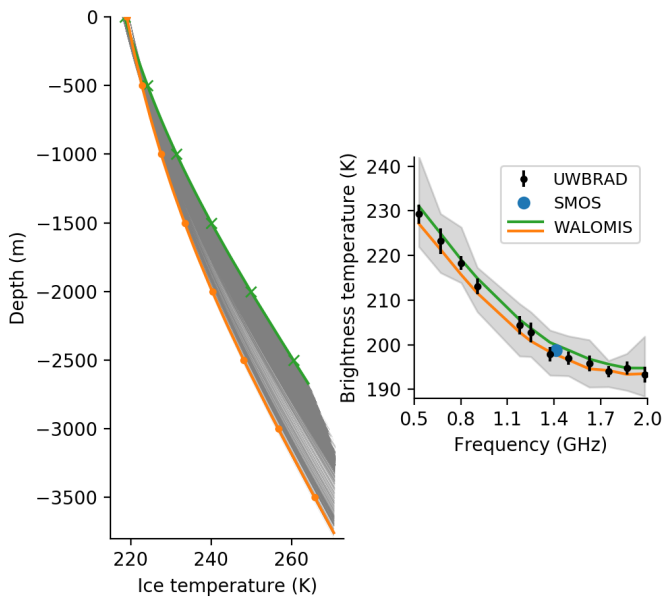


Fig. 5. (Left) All temperature profiles along the Dome C area flight estimated from Robin model. (Right) Mean and standard deviation UWBRAD spectrum between 0.5 and 2 GHz (black dots) in the Dome C area and minimum and maximum (pale gray). The mean SMOS brightness temperature is in blue dot. Two WALOMIS simulations examples obtained from the warmest (green) and the coldest (orange) temperature profiles reported on the left figure are provided in the respective colors.

of the radiometer. A good agreement is also observed with mean SMOS observations at the closest UWBRAD frequency at 1370 MHz (mean difference of -0.9 K), while the SMOS standard deviation is much lower (0.4 K).

IV. CONCLUSION

First airborne radiometric measurements in the range 500–2000 MHz were conducted in Antarctica within the ISSIUMAX project to confirm the potential of this instrument in inferring geophysical properties of sea ice, glaciers, and ice sheet. Here, the analysis focuses on brightness temperature measurements collected over ice sheet along a more than 1000-km path between MZS on the Ross sea and the Italian–French Concordia base on the East Antarctic Plateau. UWBRAD measurements were found to be only moderately affected by RFI, confirming the capability of this unprotected band for exploring geophysical properties at high latitudes.

Results point out that, depending on frequency, brightness temperature is sensitive to the temperature of a different portion of the ice sheet because of the different penetration depth. Comparisons of measured and modeled data show reasonable agreement and validate the measurement’s sensitivity to temperature deep within the ice sheet. Investigations into the raster flight over the Dome C area further show the stability of the UWBRAD radiometer. Measurements at L-band were also in agreement with SMOS observations highlighting the good absolute calibration of the radiometer at this frequency.

Finally, ISSIUMAX flights also surveyed coastal scenes including sea ice and glaciers for which analyses will be reported in future papers.

REFERENCES

- [1] G. Macelloni, M. Leduc-Leballeur, F. Montomoli, M. Brogioni, C. Ritz, and G. Picard, “On the retrieval of internal temperature of antarctica ice sheet by using smos observations,” *Remote Sens. Environ.*, vol. 233, p. 111405, 2019.
- [2] S. Tan, M. Aksoy, M. Brogioni, G. Macelloni, M. Durand, K. C. Jezek, T.-L. Wang, L. Tsang, J. T. Johnson, M. R. Drinkwater, and L. Brucker, “Physical models of layered polar firn brightness temperatures from 0.5 to 2 ghz,” *IEEE J. Sel. Top. Appl. Earth Obs. Remote Sens.*, vol. 8, no. 7, pp. 3681–3691, 2015.
- [3] K. C. Jezek, J. T. Johnson, M. R. Drinkwater, G. Macelloni, L. Tsang, M. Aksoy, and M. Durand, “Radiometric approach for estimating relative changes in intraglacier average temperature,” *IEEE Trans. Geosci. Remote Sens.*, vol. 53, no. 1, pp. 134–143, 2015.
- [4] C. Yardim, J. T. Johnson, K. C. Jezek, M. Andrews, M. Durand, Y. Duan, S. Tan, L. Tsang, M. Brogioni, G. Macelloni, and A. Bringer, “Greenland ice sheet subsurface temperature estimation using ultrawideband microwave radiometry,” *IEEE Trans. Geosci. Rem. Sens.*, 2020.
- [5] M. J. Andrews, J. T. Johnson, K. C. Jezek, H. Li, A. Bringer, C.-C. Chen, D. J. Belgiovane, V. Leuski, G. Macelloni, and M. Brogioni, “The ultrawideband software-defined microwave radiometer: Instrument description and initial campaign results,” *IEEE Trans. Geosci. Remote Sens.*, vol. 56, no. 10, pp. 5923–5935, 2018.
- [6] K. C. Jezek, J. T. Johnson, S. Tan, L. Tsang, M. J. Andrews, M. Brogioni, G. Macelloni, M. Durand, C. Chen, D. J. Belgiovane, Y. Duan, C. Yardim, H. Li, A. Bringer, V. Leuski, and M. Aksoy, “500–2000-mhz brightness temperature spectra of the northwestern greenland ice sheet,” *IEEE Trans. Geosci. Remote Sens.*, vol. 56, no. 3, pp. 1485–1496, 2018.
- [7] K. C. Jezek, “Observing the antarctic ice sheet using the radarsat-1 synthetic aperture radar,” *Polar Geogr.*, vol. 27, no. 3, pp. 197–209, 2003.
- [8] M. Andrews, J. T. Johnson, M. Brogioni, G. Macelloni, and K. Jezek, “Properties of the 500-2000 mhz rfi environment observed in high latitude airborne radiometer measurements,” *in prep. for IEEE Trans. Geosci. Rem. Sens.*, 2020.
- [9] J. T. Johnson, “An efficient two-scale model for the computation of thermal emission and atmospheric reflection from the sea surface,” *IEEE Trans. Geosci. Remote Sens.*, vol. 44, no. 3, pp. 560–568, 2006.
- [10] M. Leduc-Leballeur, G. Picard, A. Mialon, L. Arnaud, E. Lefebvre, P. Possenti, and Y. Kerr, “Modeling l-band brightness temperature at dome c in antarctica and comparison with smos observations,” *IEEE Trans. Geosci. Remote Sens.*, vol. 53, no. 7, pp. 4022–4032, 2015.
- [11] A. Al Bitar, A. Mialon, Y. Kerr, F. Cabot, P. Richaume, E. Jacquette, A. Quesney, A. Mahmoodi, S. Tarot, M. Parrons, A. Al-yaari, T. Pellarin, N. Rodriguez-Fernandez, and J.-P. Wigneron, “The global smos level 3 daily soil moisture and brightness temperature maps,” *Earth Syst. Sci. Data*, vol. 9, no. 1, pp. 293–315, 2017.
- [12] H. Fréville, E. Brun, G. Picard, N. Tatarinova, L. Arnaud, C. Lanconelli, C. Reijmer, and M. Van den Broeke, “Using modis land surface temperatures and the crocus snow model to understand the warm bias of era-interim reanalyses at the surface in antarctica,” *The Cryosphere*, vol. 8, no. 4, pp. 1361–1373, 2014.
- [13] M. Morlighem, E. Rignot, T. Binder, D. Blankenship, R. Drews, G. Eagles, O. Eisen, F. Ferraccioli, R. Forsberg, P. Fretwell *et al.*, “Deep glacial troughs and stabilizing ridges unveiled beneath the margins of the antarctic ice sheet,” *Nat. Geosci.*, vol. 13, no. 2, pp. 132–137, 2020.
- [14] G. D. Q. Robin, “Ice movement and temperature distribution in glaciers and ice sheets,” *J. Glaciol.*, vol. 2, no. 18, pp. 523–532, 1955.
- [15] G. Macelloni, M. Leduc-Leballeur, M. Brogioni, C. Ritz, and G. Picard, “Analyzing and modeling the SMOS spatial variations in the east antarctic plateau,” *Remote Sens. Environ.*, vol. 180, pp. 193–204, 2016.
- [16] C. Agosta, C. Amory, C. Kittel, A. Orsi, V. Favier, H. Gallée, M. R. van den Broeke, J. Lenaerts, J. M. van Wessem, W. J. van de Berg *et al.*, “Estimation of the antarctic surface mass balance using the regional climate model mar (1979-2015) and identification of dominant processes,” *The Cryosphere*, vol. 13, no. 1, pp. 281–296, 2019.
- [17] C. Fox Maule, M. E. Purucker, N. Olsen, and K. Mosegaard, “Heat flux anomalies in antarctica revealed by satellite magnetic data,” *Science*, vol. 309, no. 5733, pp. 464–467, 2005.
- [18] R. D. West, D. P. Winebrenner, L. Tsang, and H. Rott, “Microwave emission from density-stratified antarctic firn at 6 cm wavelength,” *J. Glaciol.*, vol. 42, no. 140, pp. 63–76, 1996.
- [19] L. Tsang, J. Kong, and R. Shin, *Theory of microwave remote sensing*. Wiley-Interscience, 1987.